RESEARCH ARTICLE

Brain Pathology

Understanding the pathogenic mechanisms and therapeutic effects in neurocysticercosis

Gino Castillo[1] | Lizbeth Fustamante[1] | Ana D. Delgado-Kamiche[1,2] |
Rogger P. Camen-Orozco[1,2] | Taryn Clark[3,4] | Edson Bernal[1] |
Jemima Morales-Alvarez[1] | Maria Ferrufino[5] | Javier Mamani-Palomino[6] |
Javier A. Bustos[7] | Hector H. Garcia[8] | Cesar M. Gavidia[9] | Robert H. Gilman[3] |
Manuela Verastegui[1,10] | Cysticercosis Working Group in Peru

[1]Infectious Diseases Laboratory Research-LID, Facultad de Ciencia e Ingeniería, Universidad Peruana Cayetano Heredia, Lima, Peru

[2]Solomon H. Snyder Department of Neuroscience, Johns Hopkins University School of Medicine, Baltimore, United States

[3]The Department of International Health, Bloomberg School of Hygiene and Public Health, Johns Hopkins University, Baltimore, Maryland, USA

[4]Department of Emergency Medicine, SUNY Downstate Medical Center, Kings County Hospital Medical Center, Brooklyn, New York, New York, United States

[5]Department of Translational Molecular Pathology, The University of Texas MD Anderson Cancer Center, Houston, Texas, USA

[6]Facultad de Medicina Veterinaria y Salud animal, Universidad Peruana Cayetano Heredia, Lima, Peru

[7]Center for Global Health, Universidad Peruana Cayetano Heredia, Lima, Peru

[8]Cysticercosis Unit, Instituto Nacional de Ciencias Neurológicas, Lima, Peru

[9]School of Veterinary Medicine, Universidad Nacional Mayor de San Marcos, Lima, Peru

[10]Asociación Benéfica Prisma, Lima, Peru

Correspondence
Manuela Verastegui, Infectious Diseases Laboratory Research-LID, Facultad de Ciencia e Ingeniería, Universidad Peruana Cayetano Heredia, Lima, Peru.
Email: manuela.verastegui@upch.pe

Abstract

Despite being a leading cause of acquired seizures in endemic regions, the pathological mechanisms of neurocysticercosis are still poorly understood. This study aims to investigate the impact of anthelmintic treatment on neuropathological features in a rat model of neurocysticercosis. Rats were intracranially infected with *Taenia solium* oncospheres and treated with albendazole + praziquantel (ABZ), oxfendazole + praziquantel (OXF), or untreated placebo (UT) for 7 days. Following the last dose of treatment, brain tissues were evaluated at 24 h and 2 months. We performed neuropathological assessment for cyst damage, perilesional brain inflammation, presence of axonal spheroids, and spongy changes. Both treatments showed comparable efficacy in cyst damage and inflammation. The presence of spongy change correlated with spheroids counts and were not affected by anthelmintic treatment. Compared to white matter, gray matter showed greater spongy change (91.7% vs. 21.4%, $p < 0.0001$), higher spheroids count (45.2 vs. 0.2, $p = 0.0001$), and increased inflammation (72.0% vs. 21.4%, $p = 0.003$). In this rat model, *anthelmintic treatment destroyed* brain parasitic cysts at the cost of local inflammation similar to what is described in human neurocysticercosis. Axonal spheroids and spongy changes as markers of damage were topographically correlated, and not affected by anthelmintic treatment.

KEYWORDS
anthelmintics, axonal swelling, neurocysticercosis, neuropathology, Peru, spheroids

1 | INTRODUCTION

Neurocysticercosis (NCC) is a parasitic infection of the central nervous system caused by a larva of the pork tapeworm *Taenia solium*. Classified as a Neglected Tropical Disease by the World Health Organization (WHO), it is endemic in nations throughout Latin America, sub-Saharan Africa, and Asia, with a particularly high prevalence among economically disadvantaged populations [1]. NCC causes significant morbidity worldwide and is a major etiology for acquired epilepsy, with around 30% of cases of epilepsy [2, 3].

Clinical complications of NCC are associated with an exacerbated immune response [4], which depends on the degree of parasite contact with parenchyma [5], as well as its location in either gray or white matter. This accentuated response was observed in a viral model for multiple sclerosis, where the lesion develops from the axons (inside) to the myelin (outside), that is, lesions in the gray matter preceded demyelinating lesions [6].

An important contributor to neuroinflammation occurs after anthelmintic treatment [7]. The mainstay of treatment for the parenchymal disease is albendazole (ABZ), or more recently, ABZ with praziquantel (PZQ). Combined anthelmintic treatment has been proposed to improve drug efficacy as ABZ plus PZQ is more effective than ABZ alone in achieving cyst resolution [8, 9]. Treatment, however, may not eliminate the cyst, even using ABZ with PZQ. Another possible alternative to ABZ is oxfendazole (OXF), which is currently approved for animal use [10, 11] and is under clinical trial research [12, 13]. Our rat model provides a new approach to discovering novel neuropathological insights associated with neurocysticercosis, resulting in a low cost-effective, and physiologically relevant model [14, 15].

This study aimed to analyze how anthelmintic treatment with ABZ + PZQ or with OXF + PZQ affects neuropathological features such as gliosis, inflammatory infiltrate, and neuron damage visualized as spheroids and spongy change (SC) using the rat model of neurocysticercosis. We provided evidence of limited effect of the anthelmintic treatment on the axonal swelling and SC and the sensitive role of gray matter in NCC pathology.

2 | MATERIALS AND METHODS

2.1 | Rat intracranial infection

Holtzman rats ($n = 120$), between 10 and 14 days old, were infected with activated *Taenia solium* oncospheres, and 85/120 developed less than 4 cysticerci. Briefly,

500 activated oncospheres were suspended in 100 μL of sterile physiological salt solution (0.9%), and injected intracranially (2 mm depth at the bregma) using a 1 mL syringe and a 25-gauge needle [14], following a protocol approved by the main IACUC of the Universidad Peruana Cayetano Heredia System (SIDISI #66826, Lima, Peru).

2.2 | Anthelmintic treatment

Out of 85 infected rats, they were randomly assigned, based on MRI scan (Figure S1), to anthelmintic treatment groups as follows: (a) 30 mg/kg/day albendazole combined with 100 mg/kg/day praziquantel for 7 days, followed by an additional 7 days with only 30 mg/kg/day albendazole (ABZ), (b) 100 mg/kg/day oxfendazole combined with 100 mg/kg/day praziquantel for 7 days (OXF), or (c) untreated with only vehicle solution (0.5% carboxymethylcellulose +10% Tween-80), for the untreated group (UT). Rats were subjected to gavage treatment in two divided doses per day. Three months after the initial infection, the treatment groups (ABZ, OXF, or UT) were divided into two strata each to determine early and late pathological changes: one to be sacrificed 24 h after last dose received ($n = 17$, ABZ; $n = 14$, OXF; $n = 15$, UT), and the second stratum to be sacrificed 2 months after last dose received ($n = 13$, ABZ; $n = 15$, OXF; $n = 11$, UT). A group of uninfected animals ($n = 80$) were also included.

2.3 | Tissue processing

Brain sections were cut at a 4-μm in thickness and stained with hematoxylin and eosin (HE) every 20 sections until the scolex or maximum cyst diameter was identified. Subsequently, adjacent sections were stained with Masson's trichrome staining to detect fibrosis. The location of cysticerci within the rat brain was determined by referring to the rat brain atlas [16] to identify parenchymal, meningeal, or ventricular cysticerci.

2.4 | Immunohistochemistry

The paraffin sections were processed as previously published [17]. Briefly, slides were incubated for 1 h for protein blocking, followed by incubation with to the corresponding primary antibodies: anti-Iba-1 (Ionized calcium-binding adaptor molecule 1), and CD68 for microglia, anti-glial fibrillary acidic protein (GFAP) for

astrocytes, and anti-200 KDa heavy phosphorylated neurofilament (NFPH) for axon identification. Afterward, the sections were rinsed and incubated with their respective secondary antibodies. Sections were revealed using diaminobenzidine (DAB, Dako), counterstained with hematoxylin, and mounted in Entellan solution (Merck).

2.5 | Quantification of axonal spheroids

Immunohistochemical analysis for NFPH was used to evaluate axonal spheroids around each cysticercus, extending up to ~2000 μm from the cyst capsule in brain parenchyma (at 400× magnification). Spheroids are well-defined oval bodies (with regular borders) measuring 10–50 μm in size, lacking a nucleus. These structures stained darkly with NFPH as previously described [15]. Spheroids were counted for each cysticercus and expressed as the mean ± SEM.

2.6 | Neuropathological assessment of the lesion surrounding the cysticercus

2.6.1 | Cyst damage

Cyst damage assessment involved the utilization of light microscopy through HE staining, Masson's trichrome staining, and Iba-1 to determine the extent of disruption of the cysticercus membrane. Other alterations within the parasite including calcification, fibrosis, spiral channel degeneration, or infiltration by inflammatory cells, were also evaluated using the same staining techniques. Overall, the severity of cyst damage was categorized into three levels: (a) Healthy, characterized by a well-defined tegument, preserved spiral channel, and intact scolex; (b) Moderate, exhibiting mild to severe tegument disruption (resulting in fusion with brain parenchyma or disorganized cellular nuclei), subtle subtegumental damage (vacuolation, infiltration of inflammatory cells), evident dilatation of the spiral channel, or scolex loss; or (c) Severe, marked by complete tegument loss, accompanied by extensive subtegumental alteration (including loss of excretory canaliculi); the parasite might display fibrosis and/or calcification. A calcified cyst demonstrated severe cyst damage with dense basophilic regions (calcifications) in the tegument and scolex of the parasite. A trained pathologist, blinded to treatment group allocation and time point, examined the slides.

2.6.2 | Inflammation

To evaluate the inflammatory response within brain tissue in our rat model, we devised an inflammatory score (IS) based on microscopic observations using HE, Iba-1, and GFAP staining to detect inflammatory cells, along with Masson's trichrome staining to assess fibrosis. The analysis entailed a visual examination of the complete area surrounding each cyst (~2000 μm) in coronal sections under light microscopy with 40× objective [18, 19]. Our categorical analysis established four degrees of the IS to be assigned to each cyst, and defined as follows: (a) IS0—indicating minimal inflammatory infiltrate (<25 inflammatory cells/40× field); (b) IS1—representing moderate to severe inflammatory infiltrates (>25 inflammatory cells/40× field); (c) IS2—denoting the presence of epithelioid macrophages in contact with the cyst, but lacking evident granuloma or multinucleated giant cells; and (d) IS3—indicating the presence of granulomas and/or multinucleated giant cells.

2.6.3 | Spongy change

Since SC is commonly observed in the rat model of neurocysticercosis, we developed a SC score. This scoring system relied on Masson's Trichrome staining to quantify the extent of vacuolar disruption surrounding each cyst. The spongy change, characterized by parenchymal loss, was classified using ImageJ 1.48v software, leading to the establishment of four categories as follows: (a) SC0—indicating healthy parenchyma (0%–2% vacuolar disruption), where the vacuolar changes detected in ImageJ within the healthy parenchyma might correspond to factors like blood vessels, non-pathological edema, or the result of myelin dissolution artifacts during fixation; (b) SC1—representing minimal spongy alteration (2%–4%); (c) SC2—denoting moderate spongy alteration (4%–8%); and (d) SC3—representing severe spongy alteration (>8%).

Furthermore, we recorded the proportion of white matter encompassing each cysticercus under microscopic observation. This adjustment facilitated the consideration of potential variations in host response between gray and white matter regions.

2.7 | Statistical analysis

Count data from axonal spheroids were expressed as means with the standard error of the mean, while categorical data from SC score, the inflammatory score, or the cyst damage score were shown as percentages for each respective category. For spheroids, the data were analyzed with the Dunn test, while for categorical variables were analyzed using an ordinal logistic regression, with treatment and white matter as predictor variables. Supplementary tables included predicted percentages for each regression (for spongy change, inflammation, or cyst damage) or predicted means (for spheroids) with a 95% confidence interval using robust estimation for variance–

covariance matrix. Statistical significance was determined with a *p*-value of less than 0.05. All analyses were performed using STATA 14.0 software.

3 | RESULTS

3.1 | Albendazole and oxfendazole successfully model cyst degeneration in the rat neurocysticercosis model

We examined brain histological changes after two times points of anthelmintic treatment in the NCC model using *Taenia solium*. We wanted to explore early inflammatory conditions at 24 h after receiving the last dose, and chronic inflammatory response at 2 months after the two different anthelmintic treatments: ABZ + PZQ or OXF+ PZQ (Figure 1A). We classified cyst damage based on cyst tegument and scolex morphology, comparable to three different damage scores were considered: healthy, moderate, and severe (Figure 1B). Most brain cysts in the untreated animals presented healthy tegument and few exhibited severe cyst damage in both untreated groups at 24 h or 2 months (Figure 1C, Table S2, 1.8% and 2.9%, respectively). Cyst damage was observed mainly at the scolex with spiral channel dilatation, hyaline membrane degeneration, fibrosis or scolex evagination, and focalized inflammatory response (Figure 1D). As expected, we observed increase in cyst damage in both ABZ and OXF treatments compared with the untreated rats for both time points in parenchymal cysts (Figure 1C, Table S1, 24 h, $p < 0.0001$; 2 months, $p = 0.0028$). Although, no differences in cyst damage were seen when ABZ or OXF were compared (24 h, $p = 0.126$; 2 months, $p = 0.823$). Similar cyst damage pattern distribution was observed on extra-parenchymal cysticerci (meningeal and ventricular) (Table S3). Interestingly, oxfendazole showed better performance over albendazole only at meningeal cysticerci when compared with untreated animals ($p = 0.025$ for OXF; $p = 0.057$ for ABZ at 24 h; $p = 0.001$ for OXF; $p = 0.042$ for ABZ at 2 months). Additionally, calcified cysts were only found at 2 months group (10%, $n = 5$) in either parenchymal or meningeal locations.

3.2 | Inflammatory response in neurocysticercosis following anthelmintic treatment

To examine inflammation following anthelmintic treatment in the rat brain model of neurocysticercosis, we developed an IS evaluating the inflammatory infiltrate density and the glia morphology on HE and immunohistochemical stainings (Figure 2A, Methods). In untreated groups (sham controls), the inflammation around cysticercus was characterized by focal sites of gliosis and spongy change, with a fibrous capsule lined with numerous fusiform cells, newly formed blood vessels with little perivascular infiltration, plasma cells, heterophils (rat neutrophils and/or eosinophils), and few lymphocytes (Figure 2A). In treated groups at 24 h, cysticerci showed moderate infiltration and few cases of epithelioid macrophages, while at 2 months group, there was marked alteration of cyst integrity with clear palisade formation or multinucleated cells (Figure 2A). Either OXF or ABZ groups exhibited higher inflammation than untreated animals at both 24 h ($p < 0.0001$, $p < 0.0001$) and 2 months ($p = 0.032$, $p = 0.001$) groups, respectively (Figure 2B, Table S1), although, with no difference between oxfendazole and albendazole group at any time point ($p = 0.421$ for 24 h, $p = 0.223$ for 2 months). Similar results were obtained when analyzed degenerated cysticerci ($p = 0.002$ for moderate cyst damage; $p < 0.0001$ for severe cyst damage). The involvement of astrocytes in the inflammatory response was unclear since infected animals from both treated and untreated groups showed similar astrogliosis observed on GFAP staining (Figure S2).

3.3 | Spheroids and spongy change are co-distributed surrounding *Taenia solium* cysticerci

We previously have reported axonal damage and SC alteration extending beyond gliosis (~ 300 μm) and up to 600 μm from cysticercus in the NCC rat model [15]. Here, we wanted to explore whether cyst degeneration or inflammatory response produced by the anthelmintic treatment could exacerbate axonal spheroid formation or increase in spongy change. We established a spongy change score (SC0–SC3) using high-contrast images obtained from Masson's Trichrome staining (Figure 3A). The SC was observed as vacuolization of the brain parenchyma, and it was mainly detected at parenchymal cysticerci and, to a lesser extent, in extra-parenchymal cysticerci ($p < 0.001$ for 24 h; $p < 0.001$ for 2 months). Spheroids were identified as oval bodies positive for NFPH staining measuring between 10 and 50 μm in diameter, and absent in uninfected animals. Interestingly, higher number of spheroids surrounding the cyst were associated with higher SC scores in untreated animals (Figure 3B, $p < 0.001$ for 24 h; $p < 0.001$ for 2 months). When compared in treated animals, we did not observe any significant differences for spheroids ($p = 0.804$ for OXF, $p = 0.864$ for ABZ), SC score ($p = 0.388$ for OXF, $p = 0.740$ for ABZ), or between time points ($p = 0.309$ for spheroids; $p = 0.980$ for spongy change). Similar results were obtained when analyzed degenerated cysticerci ($p = 0.510$ for spheroids; $p = 0.620$ for spongy change). Pathological examination revealed that certain vacuoles from the SC were outlined by the NFPH staining, suggesting vacuolations within axonal processes (Figure 3C).
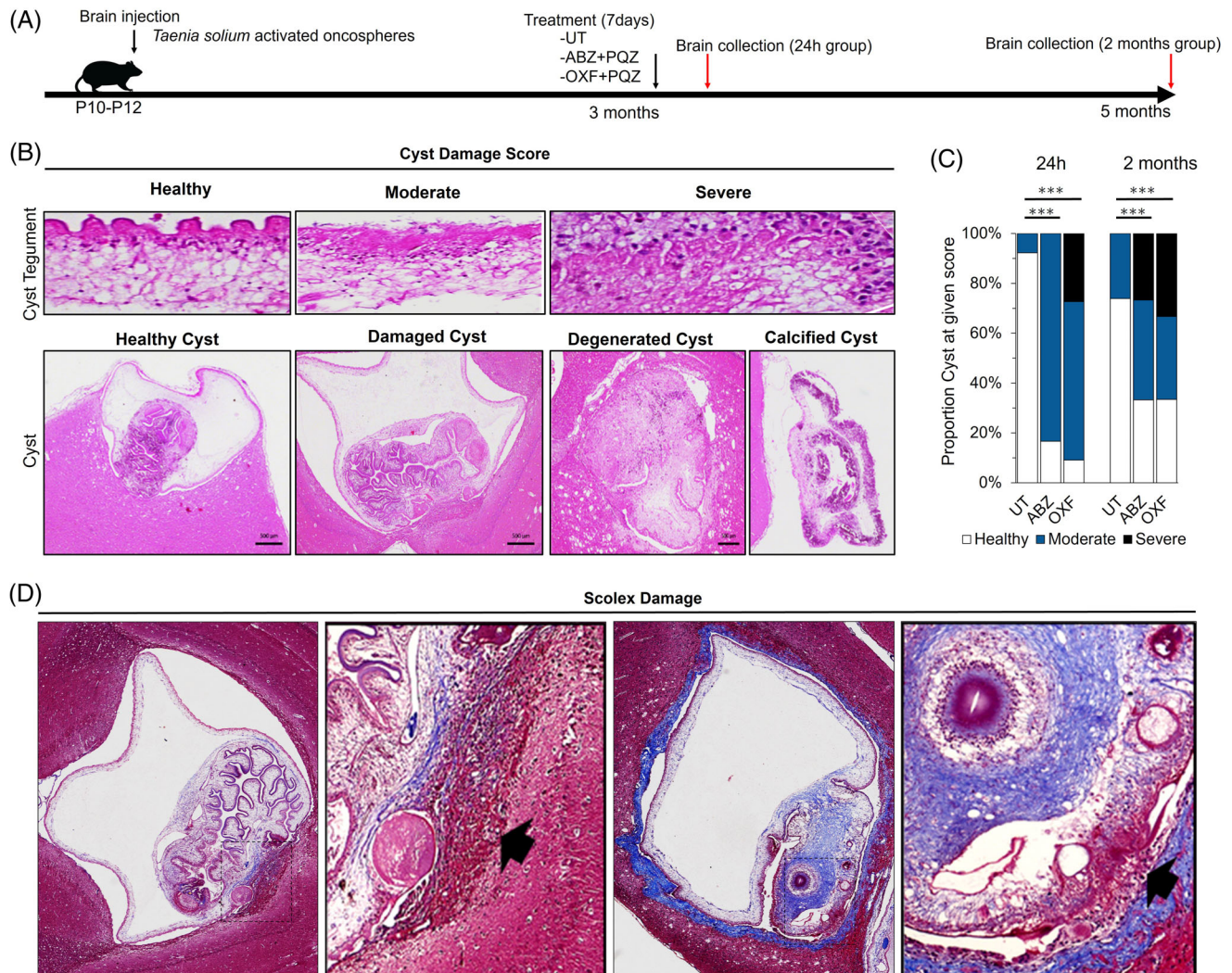
FIGURE 1 Cyst damage following anthelmintic treatment in neurocysticercosis (NCC) rat model. (A) Schematic diagram of anthelmintic treatment. Activated oncospheres were inoculated by brain injection at P10–P12 rat pups. After 3 months post-infection, rats were subjected to anthelmintic treatment with albendazole with praziquantel (ABZ), oxfendazole with praziquantel (OXF), or untreated placebo (UT) groups. Brains were collected at 24 h and 2 months following treatment. (B) Cyst damage score in rats with NCC on HE staining. Cyst tegument: Healthy, tegument and subtegument with conserved layered structures; Moderate, damage to the tegument is fused with disorganized cellular nuclei, exhibiting slight alterations in the subtegument such as vacuolation or infiltration by inflammatory cells; Severe, loss of tegument with severe subtegumental alterations, such as the loss of excretory canaliculi. Cyst: Healthy cyst, shows clear vesicular fluid with conserved membrane and scolex; Damage cyst, with focalized inflammatory response and spiral channel degeneration; Degenerated cyst, with loss of the clear fluid, altered scolex architecture (fibrosis or calcification), and thickening of parasite membrane; Calcified cyst, is observed with dense basophilic regions (calcifications) in tegument and scolex. (C) Proportion of cyst damage scores expressed as a percentage for parenchymal cysticerci following anthelmintic treatment. (***) p-value <0.0001. (D) Focalized scolex on Masson's trichrome staining. Left: Apparent vesicular cysticercus displayed a localized inflammatory response (arrow) near the scolex (square). Right: Evaginated scolex showing fibrosis (square), accompanied by localized invading inflammatory cells (arrow) and focalized loss of tegument integrity.

3.4 | Gray matter develops more severe neuropathological changes than white matter in neurocysticercosis

We observed that cyst damage and histopathological changes were not homogeneous around the cysticerci. Most lesions were found in brain areas where the cyst is surrounded by gray matter compared to white matter. Gray matter areas in contact with cysticerci showed severe SC and spheroids compared with white matter areas (Figure 4A, left). However, we detected some minor axonal swellings or varicosities (<10 μm) in white matter (Figure 4A, right). White matter areas also showed less SC (21.4% vs. 91.7%, $p < 0.0001$), spheroids (mean of 0.2 vs. 45.9, $p = 0.0001$), or inflammation (21.4% vs. 72.0%, $p = 0.003$) than gray matter in parenchymal cysticerci and none of these histopathological changes was detected in uninfected animals (Figure 4B).
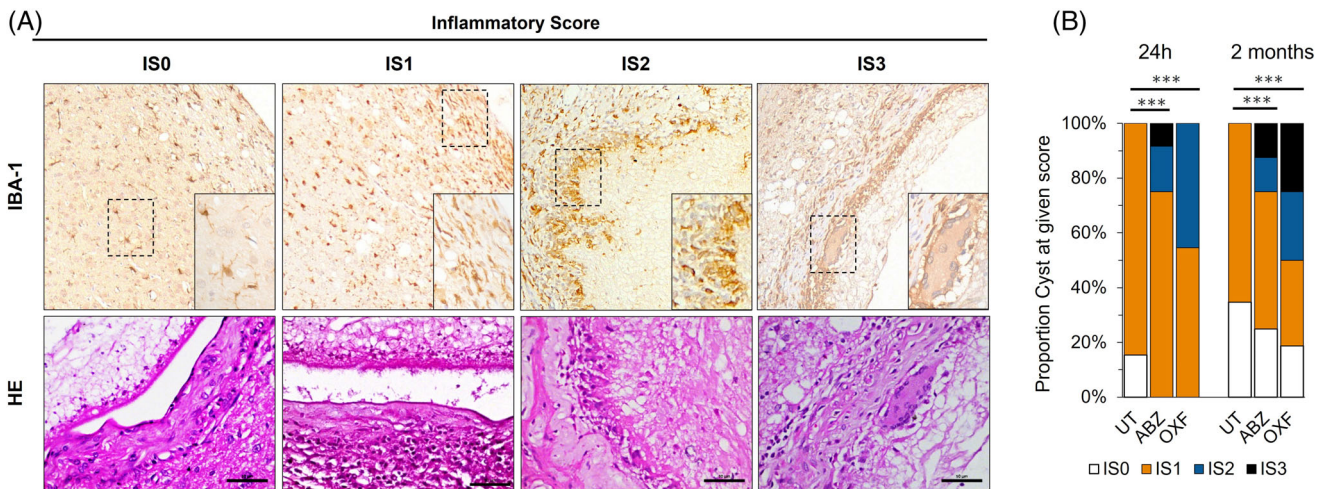
FIGURE 2 Inflammatory response in the brain tissue surrounding the cyst following anthelmintic treatment. (A) Inflammatory score in rats with neurocysticercosis assessed using Iba-1 immunohistochemistry and HE staining. IS0, cyst surrounded with minimal infiltration (<25 inflammatory cells/40× field); IS1, moderate to severe infiltration (>25 inflammatory cells/40× field) with scar formation around the cyst; IS2, epithelioid macrophages surrounding the cyst, without granulomas; IS3, granulomatous response and/or identification of multinucleated giant cells in the scar surrounding the cyst. (B) Proportion of inflammatory scores expressed as a percentage for parenchymal cysticerci following anthelmintic treatment. Rats were exposed to albendazole + praziquantel (ABZ), oxfendazole + praziquantel (OXF), or an untreated placebo (UT). (***) *p*-value <0.0001.

4 | DISCUSSION

We demonstrated that both anthelmintic treatments exhibited similar efficacy in terms of cyst damage and inflammation. However, neither treatment nor cyst damage resulted in alterations to axonal spheroids or spongy changes. This study is the first to unveil a connection between of axonal spheroids with the SC in NCC, predominantly observed within the gray matter. Spheroids represent focal swellings on degenerating axons often filled with cellular debris, including organelles, pathological proteins, and disorganized cytoskeletal elements. Accumulation of cytoskeletal elements such as NFPH, along with pathological proteins like amyloid precursor protein, superoxide dismutase, or ubiquitin, has been identified in the rat model of NCC [15]. Axonal swellings have been linked to increased seizure frequency, the most prevalent symptoms in NCC, as well as cognitive, behavioral, perceptual, and sensory-motor impairments [20]. They are associated with disorders like Seitelberger's disease [21, 22], infantile neuroaxonal dystrophy [23], cerebral malaria [24, 25], traumatic brain injury [26], Hallervorden-Spatz Syndrome [27], and Alzheimer's disease [28]. In our rat model of neurocysticercosis, rats develop around 9% seizures observed as tonic–clonic manifestations. However, the precise triggers for seizures and the link between these clinical features and spheroids remain unclear. It is crucial for future studies to establish correlations between the extent of spheroid formation and the development of seizures before inferring causality.

Furthermore, the persistence of spheroids despite the lack of change in inflammatory response, cyst damage post-treatment, or cyst volume (data not shown) suggests the possibility of a chronic antigen released by the parasite. This antigen could potentially induce an oxidative environment or cellular stress on neurons [29–31]. This aligns with models of chronic neurodegenerative diseases such as multiple sclerosis, where axonal swellings first emerge in gray matter regions and subsequently extend toward white matter areas during the later stages of the disease, irrespective of tissue inflammation [32]. Additionally, gray matter axons have lower myelination compared to white matter axons, potentially rendering them more susceptible to spheroid formation. It is plausible that the etiology of spheroids might initiate preferentially at nodes of Ranvier, known to be susceptible to axonal impairment [33]. As such, a comprehensive regional characterization of nodes of Ranvier, encompassing the node, paranode, or juxtanode, could offer insights into the pathogenesis of neurocysticercosis.

Despite the intensified inflammation brought about by anthelmintic treatment (Figure 2), the SC remained unaffected. However, in other studies, it has been observed in NCC patients with severe inflammation and heightened intracranial pressure [34, 35]. Moreover, it is described in cases of brain infections like *Stephanurus dentatus* [36] or *Toxoplasma gondii* [37], neurodegenerative diseases [38], metabolic disorders [39], and even rare genetic conditions [40]. The SC is thought to possibly reflect various aspects such as swollen astrocytic processes, distended extracellular spaces, vacuolated oligodendrocytes, dilated axons, or vacuoles within myelin lamellae, affecting both gray and white matter [41–43]. However, the timing of the SC in relation to the spheroidal pathology remains uncertain. Notably, in NCC, the vacuolated parenchyma within the SC displayed some NFP staining (Figure 3), and both appeared
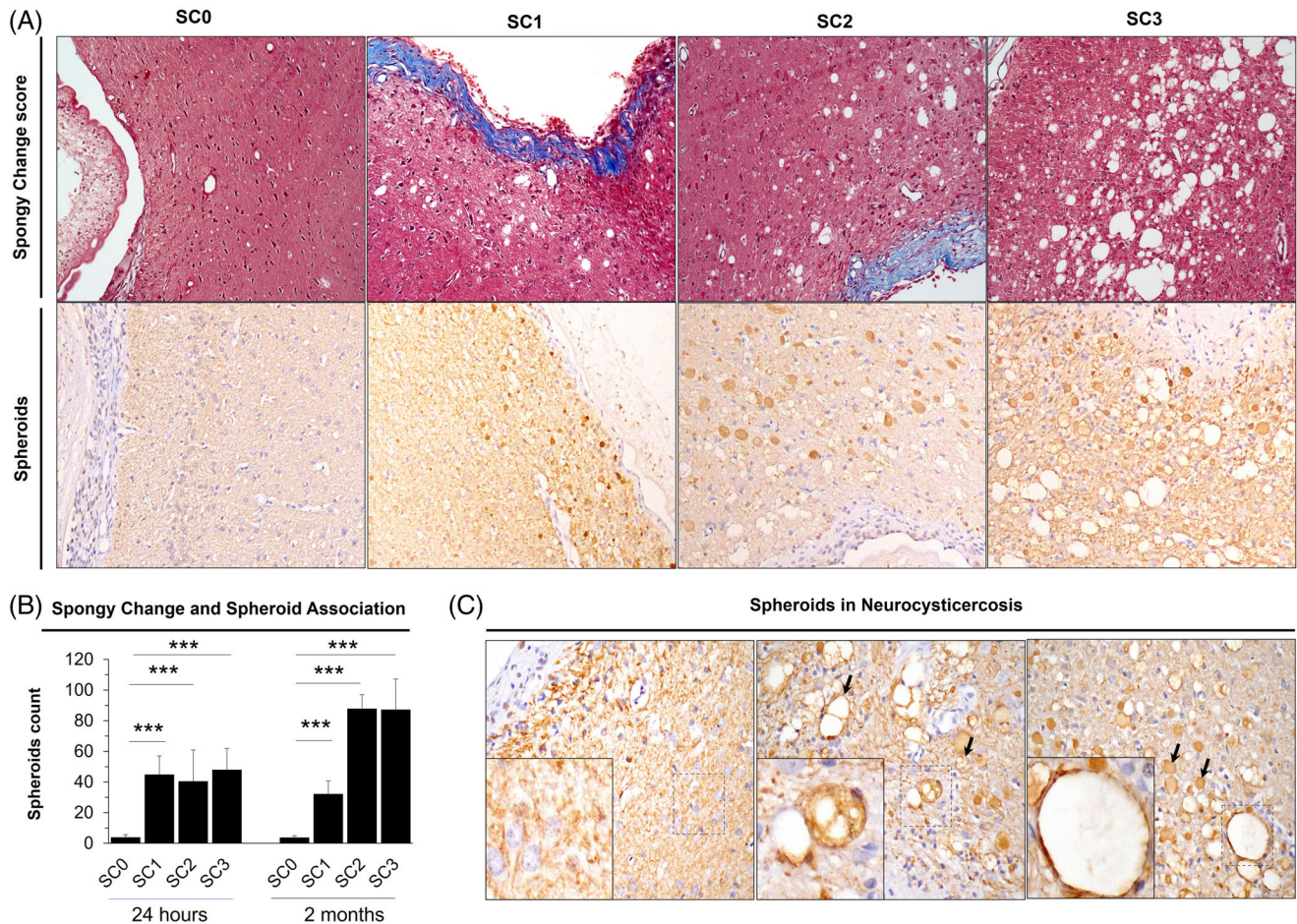
FIGURE 3 Spongy change analysis from brain tissue in neurocysticercosis (NCC) rat model. (A) Spongy change score in rats with NCC on Masson's trichrome staining. Spongy change is observed as vacuolated brain parenchyma. SC0, absence of spongy change; SC1, minimum spongy change; SC2 moderate spongy change; SC3, Severe spongy change. Corresponding immunoperoxidase staining for 200 KDa anti-neurofilament are shown below each spongy change score. (B) Association between spheroids count and spongy change score at 24 h and 2 months following treatment. Error bars represent standard error of the mean. (***) p-value <0.0001. (C) Spheroids in NCC. Spheroids are recognized as well-defined oval bodies with a regular border shape, measuring 10–50 μm in diameter. They appear darkly stained and lack a nucleus inside (arrows, right). Left, infected brain lacking spongy change and spheroids; Middle, spheroids display vacuolations within them (arrows); Right, spongy change with a stained perimeter (square), associated with spheroids (arrows).

simultaneously. This scenario could be analogous to transgenic axonal degeneration models, where the spongy change, marked by vacuolar alterations, emerged early in the proximal axons, and spanned the entire axonal caliber [44, 45]. Alternatively, SC could arise due to spheroid overgrowth leading to axonal rupture. This rupture might release pro-degenerative factors into the extracellular space, thereby contributing to neurodegeneration [46]. The association between spheroids and SC may also be observed in patients with traumatic injuries [47].

The observed inflammatory response in the rat model at the 2-months group closely resembled the pathology of human NCC. It was characterized by the presence macrophages and heterophils, with limited involvement of lymphocytes. The chronic profile included the presence of epithelioid and multinucleated giant cells, akin to the human conditions [48]. Surprisingly, even though the scolex might undergo degeneration, the tegument could

remain unaltered (Figure 1D). This observation suggests a potentially heightened antigenicity of the scolex and implies a non-essential role of the tegument for parasite survival. Exploring the underlying pathophysiology involving inflammatory cells and understanding how parasites modulate the immune response could potentially lead to novel avenues for improving therapeutics for neurocysticercosis.

The utilization of higher anthelmintic doses in this study was justified by differences in gastrointestinal absorption and the increased liver capacity for drug metabolism in rats. Furthermore, prior research has underscored the efficacy of elevated plasma concentrations of anthelmintics [49] and prolonged drug exposure [50] in achieving better outcomes in addressing extra-parenchymal cysts. These findings could potentially explain the superior effectiveness of oxfendazole compared to albendazole observed in our study (Figure 1) and in porcine
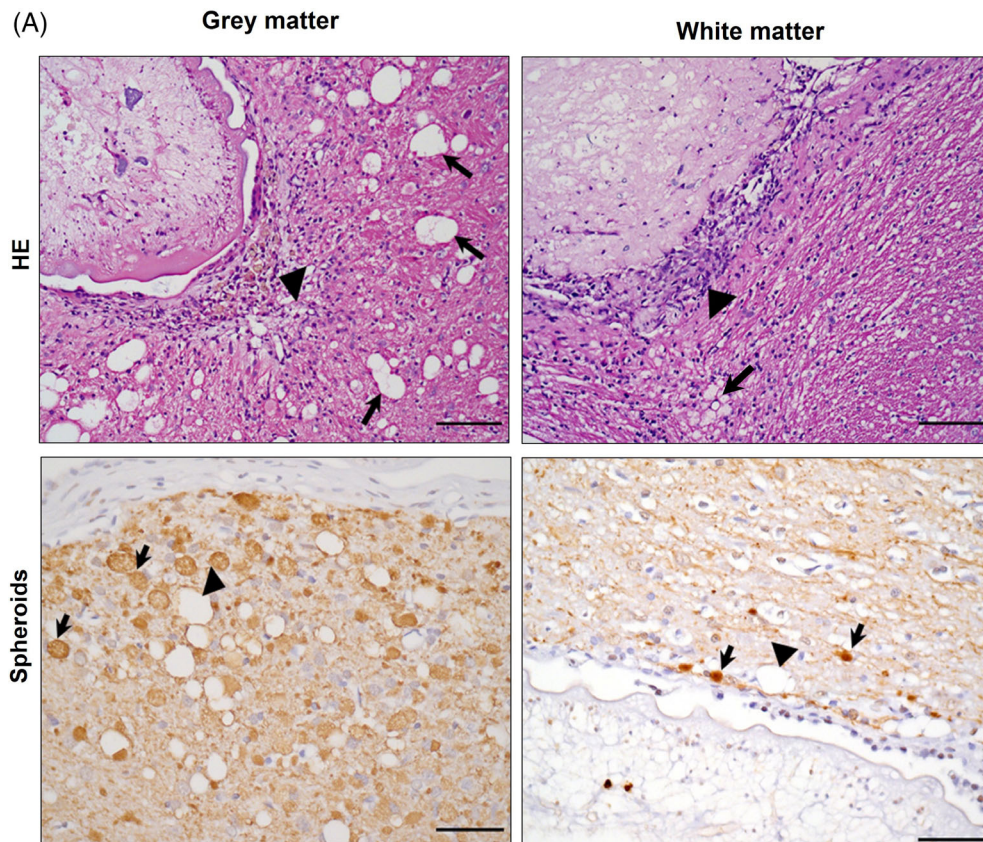
FIGURE 4 Gray and white matter associated changes in neurocysticercosis (NCC) rat model. (A) Top, HE staining on infected brain. Left, cyst surrounded by gray matter showing severe spongy change (arrows) and inflammatory infiltrate (arrowhead); Right, cyst surrounded by white matter showing slight spongy change (arrow), but inflammatory infiltrate (arrowhead). Bottom, neurofilament staining for spheroids on infected brain. Left, cyst surrounded by gray matter showing severe spongy change (arrowhead) and abundant associated spheroids (arrows); Right, cyst surrounded by white matter showing varicosities (arrows) with diameters <10 μm, and slight spongy change (arrowhead). Scale bar = 100 μm. (B) Pathological features in untreated rats within gray and white matter areas. Gray matter is the most affected area in NCC. Percentages are used to express values for spongy change (SC >0) and inflammation (IS >0), while counts for spheroids. Error bars indicate the standard error of the mean. (***) p-value <0.0001.
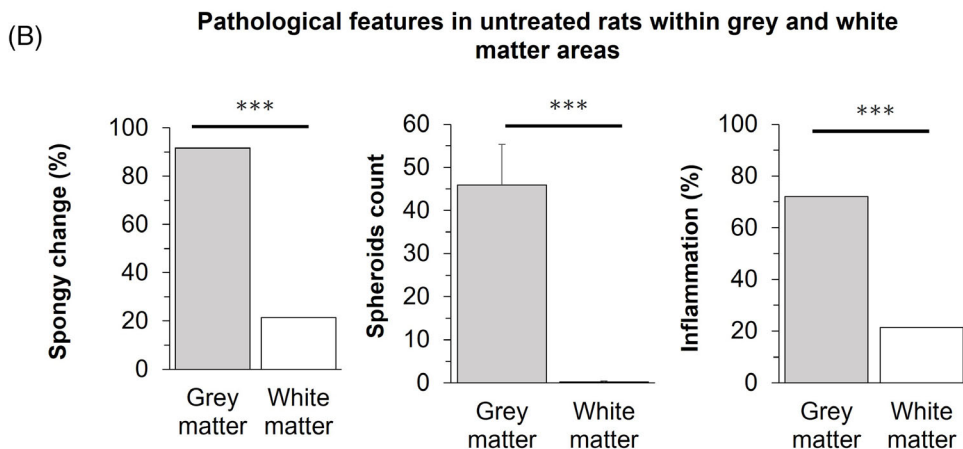
models [51, 52]. While the rat model has not previously reported such outcomes, previous reports primarily focused on comparing albendazole with praziquantel [53]. A more comprehensive examination of the inflammatory response and cellular stress might offer supplementary insights for managing this intricate disease. Additionally, an extended evaluation period should be carried out to ascertain any time-dependent reversal effects.

A key limitation of this study is the ongoing uncertainty surrounding the underlying cause of spheroid formation. It remains unknown whether spheroids serve as markers of irreversible neuronal damage or if they might repair. Further investigations utilizing larger brains and longer-living models, such as the pig cysticercosis model, hold potential to yield more definitive answers to these questions.

Moreover, the lack of association between the inflammation and the spheroids count prompts the consideration of a broader timeframe. This expanded approach would help elucidate the processes leading to spheroid formation and establish the correlation with the occurrence of spongy change.

5 | CONCLUSIONS

The study provided evidence of the distinct vulnerability between gray and white matter in neurocysticercosis. It has demonstrated the susceptibility of gray matter to inflammation, spongy change, and spheroids in neurocysticercosis. The anthelminthic treatment seemed not to influence spheroids or spongy change, but both were strongly associated with each other. The potential identification of immune factors released by the parasite could hold the key to clarifying the intricate pathogenesis of neurocysticercosis, thereby paving the way for enhanced disease management.

AUTHOR CONTRIBUTIONS

Gino Castillo, Lizbeth Fustamante, Ana D. Delgado-Kamiche, Rogger P. Camen-Orozco, Edson Bernal, and Jemima Morales-Alvarez conducted experiments. Gino Castillo, Maria Ferrufino, and Javier Mamani-Palomino performed the neuropathological assessment and data collection. Gino Castillo, Lizbeth Fustamante, Cesar M. Gavidia, and Manuela Verastegui analyzed data and performed statistical analyses. Gino Castillo, Lizbeth Fustamante, Taryn Clark, Rogger P. Carmen-Orozco and Cesar M. Gavidia prepared the manuscript. Lizbeth Fustamante and Edson Bernal contributed to the overall direction of the treatment study. Hector H. Garcia, Cesar M. Gavidia, Manuela Verastegui, and Robert H. Gilman conceived the study, supervised the experiment, and critically revised the manuscript. All authors read and approved the final manuscript.

CONFLICT OF INTEREST STATEMENT

The authors declare that they have no conflict of interest.

DATA AVAILABILITY STATEMENT

All databases will be available in an open repository after the manuscript is accepted.

ETHICS STATEMENT

All experimental procedures in this study were approved by Institutional Animal Care and Use Committee from Universidad Peruana Cayetano Heredia (UPCH) and performed following the National Institutes of Health Guide for the Care and Use of Laboratory Animals.

ORCID

Gino Castillo https://orcid.org/0000-0001-5997-5206
Robert H. Gilman https://orcid.org/0000-0002-9037-0712

Manuela Verastegui https://orcid.org/0000-0002-7500-1353

REFERENCES

1. Donadeu M, Lightowlers MW, Fahrion AS, Kessels J, Abela-Ridder B. Taenia solium: WHO endemicity map update. Wkly Epidemiol Rec. 2016;91:595–9.
2. Debacq G, Moyano LM, Garcia HH, Boumediene F, Marin B, Ngoungou EB, et al. Systematic review and meta-analysis estimating association of cysticercosis and neurocysticercosis with epilepsy. PLoS Negl Trop Dis. 2017;11:e0005153.
3. del Brutto OH, Arroyo G, Del Brutto VJ, Zambrano M, García HH. On the relationship between calcified neurocysticercosis and epilepsy in an endemic village: a large-scale, computed tomography-based population study in rural Ecuador. Epilepsia. 2017;58:1955–61.
4. Herrick JA, Maharathi B, Kim JS, Abundis GG, Garg A, Gonzales I, et al. Inflammation is a key risk factor for persistent seizures in neurocysticercosis. Ann Clin Transl Neurol. 2018;5:630–9.
5. Cangalaya C, Zimic M, Marzal M, González AE, Guerra-Giraldez C, Mahanty S, et al. Inflammation caused by praziquantel treatment depends on the location of the *Taenia solium* cysticercus in porcine neurocysticercosis. PLoS Negl Trop Dis. 2015;9:e0004207.
6. Sato F, Tanaka H, Hasanovic F, Tsunoda I. Theiler's virus infection: pathophysiology of demyelination and neurodegeneration. Pathophysiology. 2011;18:31–41.
7. Mahanty S, Orrego MA, Mayta H, Marzal M, Cangalaya C, Paredes A, et al. Post-treatment vascular leakage and inflammatory responses around brain cysts in porcine neurocysticercosis. PLoS Negl Trop Dis. 2015;9:e0003577.
8. Monk EJM, Abba K, Ranganathan LN. Anthelmintics for people with neurocysticercosis. Cochrane Database Syst Rev. 2021;6:CD000215.
9. Garcia HH, Gonzales I, Lescano AG, Bustos JA, Zimic M, Escalante D, et al. Efficacy of combined antiparasitic therapy with praziquantel and albendazole for neurocysticercosis: a double-blind, randomised controlled trial. Lancet Infect Dis. 2014;14:687–95.
10. Bach T, Bae S, D'Cunha R, Winokur P, An G. Development and validation of a simple, fast, and sensitive LC/MS/MS method for the quantification of oxfendazole in human plasma and its application to clinical pharmacokinetic study. J Pharm Biomed Anal. 2019;171:111–7.
11. Bach T, Galbiati S, Kennedy JK, Deye G, Nomicos EYH, Codd EE, et al. Pharmacokinetics, safety, and tolerability of oxfendazole in healthy adults in an open-label phase 1 multiple ascending dose and food effect study. Antimicrob Agents Chemother. 2020;64:e01018–20. https://doi.org/10.1128/AAC.01018-20
12. An G, Murry DJ, Gajurel K, Bach T, Deye G, Stebounova LV, et al. Pharmacokinetics, safety, and tolerability of oxfendazole in healthy volunteers: a randomized, placebo-controlled first-in-human single-dose escalation study. Antimicrob Agents Chemother. 2019;63:e02255–18. https://doi.org/10.1128/AAC.02255-18
13. Gonzalez AE, Codd EE, Horton J, Garcia HH, Gilman RH. Oxfendazole: a promising agent for the treatment and control of helminth infections in humans. Expert Rev Anti Infect Ther. 2019;17:51–6.
14. Verastegui MR, Mejia A, Clark T, Gavidia CM, Mamani J, Ccopa F, et al. Novel rat model for neurocysticercosis using *Taenia solium*. Am J Pathol. 2015;185:2259–68.
15. Mejia Maza A, Carmen-Orozco RP, Carter ES, Dávila-Villacorta DG, Castillo G, Morales JD, et al. Axonal swellings

and spheroids: a new insight into the pathology of neurocysticercosis. Brain Pathol. 2019;29:425–36.

16. Watson GPC. The rat brain in stereotaxic coordinates. 6th ed. Cambridge, MA: Elsevier; 2006.

17. Carmen-Orozco RP, Dávila-Villacorta DG, Cauna Y, Bernal-Teran EG, Bitterfeld L, Sutherland GL, et al. Blood-brain barrier disruption and angiogenesis in a rat model for neurocysticercosis. J Neurosci Res. 2019;97:137–48.

18. Restrepo BI, Alvarez JI, Castaño JA, Arias LF, Restrepo M, Trujillo J, et al. Brain granulomas in neurocysticercosis patients are associated with a Th1 and Th2 profile. Infect Immun. 2001;69: 4554–60.

19. Sikasunge CS, Johansen MV, Phiri IK, Willingham AL 3rd, Leifsson PS. The immune response in Taenia solium neurocysticercosis in pigs is associated with astrogliosis, axonal degeneration and altered blood-brain barrier permeability. Vet Parasitol. 2009; 160:242–50.

20. Maia PD, Hemphill MA, Zehnder B, Zhang C, Parker KK, Kutz JN. Diagnostic tools for evaluating the impact of focal axonal swellings arising in neurodegenerative diseases and/or traumatic brain injury. J Neurosci Methods. 2015;253:233–43.

21. Gordon N. Infantile neuroaxonal dystrophy (Seitelberger's disease). Dev Med Child Neurol. 2002;44:849–51.

22. Scheithauer BW, Forno LS, Dorfman LJ, Kane CA. Neuroaxonal dystrophy (Seitelberger's disease) with late onset, protracted course and myoclonic epilepsy. J Neurol Sci. 1978;36:247–58.

23. Riku Y, Ikeuchi T, Yoshino H, Mimuro M, Mano K, Goto Y, et al. Extensive aggregation of α-synuclein and tau in juvenile-onset neuroaxonal dystrophy: an autopsied individual with a novel mutation in the PLA2G6 gene-splicing site. Acta Neuropathol Commun. 2013;1:12.

24. Idro R, Marsh K, John CC, Newton CR. Cerebral malaria: mechanisms of brain injury and strategies for improved neurocognitive outcome. Pediatr Res. 2010;68:267–74.

25. Medana IM, Day NP, Hien TT, Mai NT, Bethell D, Phu NH, et al. Axonal injury in cerebral malaria. Am J Pathol. 2002;160: 655–66.

26. Sahuquillo J, Vilalta J, Lamarca J, Rubio E, Rodriguez-Pazos M, Salva JA. Diffuse axonal injury after severe head trauma. A clinico-pathological study. Acta Neurochir (Wien). 1989;101:149–58.

27. Gothwal S, Nayan S. Hallervorden-Spatz syndrome with seizures. Basic Clin Neurosci. 2016;7:165–6.

28. Born HA. Seizures in Alzheimer's disease. Neuroscience. 2015; 286:251–63.

29. Fang C, Bourdette D, Banker G. Oxidative stress inhibits axonal transport: implications for neurodegenerative diseases. Mol Neurodegener. 2012;7:29.

30. Wali G, Liyanage E, Blair NF, Sutharsan R, Park JS, Mackay-Sim A, et al. Oxidative stress-induced axon fragmentation is a consequence of reduced axonal transport in hereditary spastic paraplegia SPAST patient neurons. Front Neurosci. 2020; 14:401.

31. Seo WM, Yoon J, Lee J-H, Lee Y, Lee H, Geum D, et al. Modeling axonal regeneration by changing cytoskeletal dynamics in stem cell-derived motor nerve organoids. Sci Rep. 2022;12:2082.

32. Tsunoda I, Kuang L-Q, Libbey JE, Fujinami RS. Axonal injury heralds virus-induced demyelination. Am J Pathol. 2003;162: 1259–69.

33. Edgar JM, McLaughlin M, Yool D, Zhang SC, Fowler JH, Montague P, et al. Oligodendroglial modulation of fast axonal transport in a mouse model of hereditary spastic paraplegia. J Cell Biol. 2004;166:121–31.

34. Rangel R, Torres B, del Bruto O, Sotelo J. Cysticercotic encephalitis: a severe form in young females. Am J Trop Med Hyg. 1987;36: 387–92.

35. Srinivas HV, Rao TV, Deshpande DH. Cerebral cysticercosis: clinical and pathological observations with emphasis on the encephalitic type. Clin Neurol Neurosurg. 1980;82:187–97.

36. Prado RGS, Gardiner CH, Moura MAO, Gonzalez GBE, Duarte MD, Santos TFS, et al. Parasitic encephalitis caused by Stephanurus dentatus in a pig in Brazil. J Vet Diagn Invest. 2021; 33:949–51.

37. Tang TT, Harb JM, Dunne WM Jr, Wells RG, Meyer GA, Chusid MJ, et al. Cerebral toxoplasmosis in an immunocompromised host: a precise and rapid diagnosis by electron microscopy. Am J Clin Pathol. 1986;85:104–10.

38. Hansen LA, Masliah E, Terry RD, Mirra SS. A neuropathological subset of Alzheimer's disease with concomitant Lewy body disease and spongiform change. Acta Neuropathol. 1989;78:194–201.

39. Seitelberger F. The problem of status Spongiosus. In: Klatzo I, Seitelberger F, editors. Brain edema. Vienna: Springer; 1967. p. 152–69.

40. Gambetti P, Mellman WJ, Gonatas NK. Familial spongy degeneration of the central nervous system (Van Bogaert-Bertrand disease). Acta Neuropathol. 1969;12:103–15.

41. Lamfert PW, Schochet SS. Electron microscopic observations on experimental spongy degeneration of the cerebellar White matter. J Neuropathol Exp Neurol. 1968;27:210–20.

42. Hagen G, Bjerkås I. Spongy degeneration of white matter in the central nervous system of silver foxes (Vulpes vulpes). Vet Pathol. 1990;27:187–93.

43. Adachi M, Torii J, Schneck L, Volk BW. Electron miscroscopic and enzyme histochemical studies of the cerebellum in spongy degeneration. Acta Neuropathol. 1972;20:22–31.

44. Anderson TJ, Schneider A, Barrie JA, Klugmann M, McCulloch MC, Kirkham D, et al. Late-onset neurodegeneration in mice with increased dosage of the proteolipid protein gene. J Comp Neurol. 1998;394:506–19.

45. Sasaki S, Warita H, Abe K, Iwata M. Slow component of axonal transport is impaired in the proximal axon of transgenic mice with a G93A mutant SOD1 gene. Acta Neuropathol. 2004;107: 452–60.

46. Yong Y, Hunter-Chang S, Stepanova E, Deppmann C. Axonal spheroids in neurodegeneration. Mol Cell Neurosci. 2021;117: 103679.

47. Ellison D, Love S, Chimelli L, Harding BN, Lowe JS, Vinters HV, et al. Head and spinal injuries. In: Ellison D, Love S, Chimelli L, Harding BN, Lowe JS, Vinters HV, et al., editors. Neuropathology. 3rd ed. Oxford: Mosby; 2013. p. 271–302.

48. Lino-Junior Rde S, Faleiros AC, Vinaud MC, Oliveira FA, Guimarães JV, Reis MA, et al. Anatomopathological aspects of neurocysticercosis in autopsied patients. Arq Neuropsiquiatr. 2007;65:87–91.

49. Osorio R, Carrillo-Mezo R, Romo ML, Toledo A, Matus C, González-Hernández I, et al. Factors associated with cysticidal treatment response in extraparenchymal neurocysticercosis. J Clin Pharmacol. 2019;59:548–56.

50. White AC Jr, Coyle CM, Rajshekhar V, Singh G, Hauser WA, Mohanty A, et al. Diagnosis and treatment of Neurocysticercosis: 2017 clinical practice guidelines by the Infectious Diseases Society of America (IDSA) and the American Society of Tropical Medicine and Hygiene (ASTMH). Clin Infect Dis. 2018;66: e49–75.

51. Mkupasi EM, Ngowi HA, Sikasunge CS, Leifsson PS, Johansen MV. Efficacy of ivermectin and oxfendazole against Taenia solium cysticercosis and other parasitoses in naturally infected pigs. Acta Trop. 2013;128:48–53.

52. Sikasunge CS, Johansen MV, Willingham AL 3rd, Leifsson PS, Phiri IK. Taenia solium porcine cysticercosis: viability of cysticerci and persistency of antibodies and cysticercal antigens after treatment with oxfendazole. Vet Parasitol. 2008;158:57–66.

53. Carpio A, Kelvin EA, Bagiella E, Leslie D, Leon P, Andrews H, et al. Effects of albendazole treatment on neurocysticercosis: a randomised controlled trial. J Neurol Neurosurg Psychiatry. 2008;79: 1050–5.

SUPPORTING INFORMATION

Additional supporting information can be found online in the Supporting Information section at the end of this article.